

# Analysis of LTE Relay Interface for Self-Backhauling in LTE Mesh Networks

Romain Favraud, Navid Nikaein  
Communication Systems Department, EURECOM, France  
Email: firstname.name@eurecom.fr

**Abstract**—LTE is deployed in most countries and continuously evolving to match new user requirements. While it is expected to support 5G deployments for outdoor and long range communications, it will also be used for Public Safety services in major countries. Among those, new scenarios call for wider networks on the move relying on self-backhauling. In this article we argue that the LTE relay interface ( $Un$ ) is an efficient candidate to enable multi-hop LTE mesh networks. We first study the  $Un$  interface and highlight its main properties. We then analyze and compare out-band  $LTE-Uu$ , in-band  $LTE-Uu$  with full duplex radios and in-band  $Un$  interface to mesh LTE base stations. We perform link-level emulations to assess the performance of the  $Un$  interface subject to different conditions. Finally, we compare the achievable throughput of self-backhauled LTE mesh network using either  $Un$  or  $LTE-Uu$  through a system-level simulation.

## I. INTRODUCTION

Long Term Evolution (LTE) is now the 4G cellular network of reference. It has been adopted by all major operators over the world and is expected to rule the cellular landscape for the current decade. 3GPP LTE specifications are getting more complex, expanding its use-cases and increasing its performance and features at every new release. Although new transmission techniques and a new physical layer will probably emerge for the future 5G network, LTE is evolving to be able to address several issues (e.g. cellular networks' capacity crunch, ultra-high bandwidth, ultra-low latency, massive numbers of connections, super-fast mobility, diverse-spectrum access) and to become the 5G outdoor and long range radio access technology (RAT). Moreover, LTE is expected to play an essential role in advancing Public Safety (PS) communications and several items have been specified in this regard. In [1] and [2], several issues that Public Safety Networks (PSN) have to overcome to leverage LTE as the underlying radio technology are discussed. In particular, supporting moving cells use-cases especially when out-of-coverage from the statically deployed cellular network needs to be considered.

3GPP has defined the concept of Isolated E-UTRAN, allowing eNodeB (eNB) to continue providing minimal services for local PS users when the link to the Evolved Packet Core (EPC) is lost or disturbed. But in this case each node remains isolated from the others even when they are in radio coverage of each other. To overcome this limitation, several methods can be used to re-establish communications between nodes. Usually, additional RATs are deployed to re-establish the backhaul link [3], [4]. The development of Full Duplex (FD) radios have

triggered some studies to use it for self-backhauling in cellular networks [5], [6]. However, FD solutions require accurate calibration and are generally very expensive, and might not be suitable for high power nodes that could be embedded in PS vehicles. In LTE Rel.10, 3GPP introduced the LTE relay interface ( $Un$ ) to allow the deployment of fixed relay nodes that use in-band LTE to extend the coverage of standard eNBs by one hop and to increase the network capacity. There have been several studies showing the advantages and limitations of relay nodes but they seem not to be followed by real deployments due to changes in the telecommunication market and to the emergence of small cell architectures.

We believe that several use-cases can benefit from the meshing of the base stations (BSs) such as vehicular networking as well as disaster or emergency networks. Taking a new perspective, we presented a new BS concept (e2NB) leveraging the  $Un$  interface to create wireless mesh networks of LTE BSs relying on a LTE in-band backhaul [5], [7]. Extending this initial work, we study in this paper the  $Un$  interface in details to assess its efficiency for multi-hop LTE meshing. In section II, we recall what is a LTE relay and present the R-PDCCH (Relay Physical Downlink Control CHannel) and R-PDSCH (Relay Physical Downlink Shared CHannel) that support the  $Un$  interface. Then, we compare several approaches to realize a mesh network of LTE BSs using self-backhauling, either out-band with the legacy  $Uu$  (interface between eNB and UE), in-band using Full-Duplex radios or in-band using the  $Un$  interface. In section IV, we present our current implementation of the R-PDCCH and R-PDSCH on the OpenAirInterface (OAI) SDR platform and compare the  $Un$  interface and  $Uu$  interface link-level performance. We then compare their performance in a multi-node system-level simulation. We conclude this work based on these results and discussion before presenting the next steps of our research.

## II. LTE RELAY PHYSICAL CHANNELS

3GPP defined LTE relay nodes starting from Release 10 [8]. The LTE relay is applying a decode-and-forward relay scheme. It is connected to a Donor eNB (DeNB) that acts as its anchor point while serving LTE Release 8 (and above) UEs. Thus, a relay node includes two physical layer entities, a first one that communicates with the DeNB and a second one that communicates with the surrounding UEs. The connection between the relay and the DeNB is called the backhaul link

(DeNB ↔ relay) while the connection between the relay and the UEs is called the access link (relay ↔ UE).

LTE relay can be in-band using the same frequency band for the backhaul link and for the access link, or out-band using different frequency bands for the backhaul and access links. When used out-band, one radio is using the legacy LTE *Uu* interface to communicate with the DeNB while a second radio on a different band is also using *Uu* for the access link. However, when used in-band, the backhaul link and access link are time-division multiplexed in a single frequency band over one radio chain.

### A. *Un* interface

To fully support the *Uu* interface specifications, BSs (including relays) have to broadcast a number of mandatory control messages and synchronization signals (e.g. PSS, SSS, PBCH, SIB2 or CRS). In LTE Rel. 8, UEs are expecting CRS (Cell Reference Signals) to be transmitted in both slots of every DL SF for synchronization and channel estimation purposes. An in-band relay must be able to receive from its DeNB on the DL channel and band that it is also using to transmit its access link. Thus, 3GPP has defined a new interface for the backhaul link in that case. It is called *Un* and is described in Technical Specification (TS) 36.216. With the introduction of the eMBMS (enhanced Multimedia Broadcast Multicast Service) mechanism in Rel. 8, a new type of SF is defined, called Multicast-Broadcast Single-Frequency Network (MBSFN) SF,<sup>1</sup> where UEs are expecting the reference signals *only* in the first SF symbols (PCFICH/PHICH). Using this property, a relay can switch from TX mode to RX mode after sending the first mandatory symbols to its UEs and can use the symbols left in the SF to receive from its DeNB on the DL channel. Unfortunately, as the DeNB and the relay are in close time synchronization, the relay cannot receive the PDCCH of its DeNB and cannot infer what data resources are allocated. To overcome that, 3GPP defined a new control channel to transmit Downlink Control Indicator (DCI) to relays, called R-PDCCH. It also defined a new data channel (R-PDSCH) to cope with the fact that the relay cannot receive all the symbols of the classical PDSCH due to the propagation time and TX-RX switching time of the radio. Two main properties shared by these two channels are related to their beginning and ending in the time domain inside a SF: the first slot of a RB (resource block) can carry 4, 5 or 6 symbols and starts from *DL-StartSymbol* while the second can have 6 or 7 symbols (c.f. tables 5.4-1 and 5.4-2 of TS 36.216). The relay channel symbol length can then vary to cope with the propagation time and synchronization between the DeNB and the relay, with their number of PDCCH symbols and with their TX/RX switching time. Higher layer mechanisms are required for both entity to agree on these parameters and on others, like the resource allocation type used for R-PDCCH mapping.

1) *R-PDCCH*: It is dedicated to the transmission of relay specific DCI from the DeNB to the relay. These DCIs are

<sup>1</sup>Within each frame, there can be up to 6 MBSFN SFs in FDD, and 0 to 5 in TDD depending on the TDD configuration.

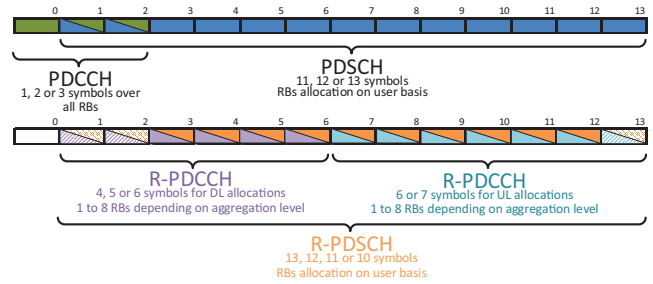


Fig. 1: SF flexibility for UE DL channels (*Uu*) (top) - relay DL channels (*Un*) (bottom)

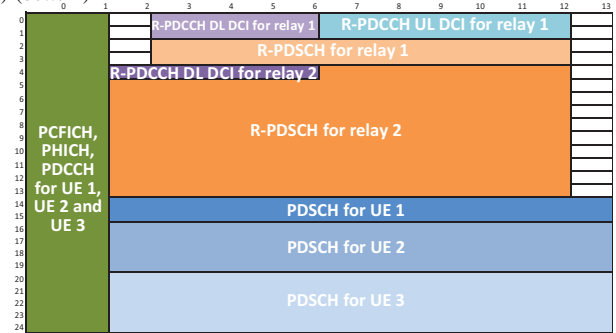


Fig. 2: Example of SF allocation from DeNB DL channel

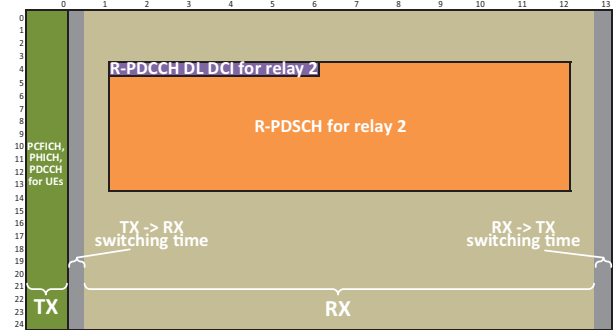


Fig. 3: Example of SF allocation for Relay DL channel shared between access and backhaul in a MBSFN SF at the relay

formatted the same way as the UE specific DCIs for legacy UEs, but the channel that transport them is mapped differently on the physical layer and their meaning for the relay can be slightly different. These DCIs are mapped on the symbols usually used to transmit the PDSCH to legacy UEs instead of being distributed over the first symbols of a SF on the PDCCH. The ePDCCH defined in LTE Rel.11 follows a similar approach. There are two types of DCIs with different R-PDCCH mapping (see Fig. 1 and 2): 1) DCI format 0, that corresponds to UL allocations, are mapped in the second slot of a SF, and 2) all the other DCIs for DL allocation are mapped on the first slot of a SF. The DeNB must give the relay a set of VRBs (virtual resource blocks) following resource allocation type 0, 1 or 2, where the DCIs have to be searched for. Interleaving and non-interleaving mapping are defined. For non-interleaving mapping, a DCI is mapped over one to eight RBs part of the VRB set depending on the aggregation level. There is a maximum of six possible positions for aggregation 0 (1 VRB) and 1 (2 VRBs), and two possible positions for aggregation 2 (4 VRBs) and 3 (8 VRBs). This gives a maximum of sixteen positions to be looked for by the relay for DL DCI. The same happens for UL DCIs in

the second slot.

2) *R-PDSCH*: R-PDSCH is similar to PDSCH. The main difference is the restriction on the symbols on which it is allocated. R-PDSCH for a specific relay is mapped from  $DL\_StartSymbol$  in the first slot and ends either at the last or penultimate symbol in the second slot (see Fig.2 and 3). This restricts the number of symbols that can vary from 12 to 10 (13 is forbidden), compared to 13 to 11 (10 for 1.4MHz channel) for legacy PDSCH. The amount of resource elements available then differs which changes the code rate for a given TBS. This might call for some change in the DL scheduler of the DeNB and the link adaptation algorithm to get similar performance than for  $Uu$ . A second difference is that the R-PDSCH allocation can overlap the resource elements carrying the DL DCI, the relay must then assume that there is no data in the first slot where the DCI is, but only in the second slot.

3) *Relay uplink*: The relay uplink (UL) channel for the backhaul link remains the same as for UEs with exception of using the last SF symbol as RX/TX switching time instead of a reference symbol. However, a relay does not expect Hybrid Automatic Repeat Request (HARQ) acknowledgment of its UL transmission over the Physical Hybrid-ARQ Indicator Channel (PHICH) as it cannot access it. It relies on explicit retransmission DCI from the DeNB or higher layer mechanisms.

4) *Relay link scheduling*: DL and UL transmissions on  $Uu$  interface are scheduled by the DeNB, but a relay can only listen to the DL channel during its MBSFN SFs. Thus, a relay and its DeNB must agree on which SFs the relay defines as MBSFN so that the DeNB does not transmit when the relay is not listening. A relay cannot schedule its UEs in the UL SFs corresponding to its DL MBSFN SFs as these UL SFs are used for the backhaul transmission to the DeNB.

5) *Hardware*: Using a relay channel calls for more hardware than classical eNBs in FDD. In TDD, it only needs a faster switching RF chain as the TX/RX switching time requirement is tighter than the one of legacy TDD. For FDD, a relay needs to transmit and receive on both DL and UL bands instead of doing only transmission on DL and reception on UL. Thus it needs two RF chains similar to TDD chains.

### III. MESHING LTE BASE STATIONS

We advocate that meshing LTE base stations is a key feature for several emerging use-cases, especially for PS. In this section, we discuss of several ways for meshing base stations based only on standardized LTE links.

#### A. Multiple LTE bands: out-band backhaul

Using multiple LTE bands at each BS is the simplest approach, and can be achieved through two settings. In a first setting, each node has the same access band and one or multiple dedicated bands for interconnections that are separated from the UE access bands. This has the advantage of keeping the UE access band unchanged to create a legacy network and leveraging the existing scheduling algorithms. In addition, a separated access band also limits the interference to the UEs belonging to the neighboring BS caused by long

range transmissions. Therefore lower transmission power can be used in conjunction with eICIC mechanisms for the access band. However, using a single backhaul band to interconnect the BSs using the  $Uu$  interface limits the number of hops from the BS to one which makes the meshing of the BSs impossible. If more than one backhaul band is used, then multiple hops between BSs are possible using only  $Uu$  through an appropriate allocation of the bands among the neighboring BSs. Relay channel could also be used on the backhaul bands with new scheduling techniques to realize more than one hop even with only one dedicated band for the backhaul. In a second setting, each BS potentially uses different access bands and connects to each neighboring node as a legacy UE on the respective access band. While more hops can be provided in this case even when using only two bands, it is subject to overlapping coverage areas, which calls for careful planning and scheduling among the adjacent nodes.

To sum up, Both solutions use multi-band access that requires additional radio chains at each node. Even if some hardware resources can be shared (antennas), isolation between the access and backhaul bands at each BS is required, which might not be possible due to regulatory constraints on getting frequency resources for each distinct band. For instance, dividing a 10MHz channel bandwidth into two 5MHz sub-bands to isolate access and backhaul will put high requirements on filters and amplifiers at each node to avoid self-interference. Furthermore, the available bandwidth will not scale with the spatio-temporal traffic variability as access and backhaul resources are completely separated, which in turn may reduce the overall performance.

#### B. Full Duplex

Full duplex radios is a trending topic as some recent advancements in analog and digital RF cancellation made their usage realistic in some scenarios [9]. Several works have been carried out to study the influence of full duplex radios on cellular systems. In [10] and [11], performance of a FD small-cell or BS on the access link with half duplex (HD) UEs is compared to the HD BS case and show interesting improvements. In [5], performance improvements are shown when using FD on small-cell relays to realize backhaul and access links at the same time. While FD radios may facilitate the establishment of the inter-BS links with a potential performance increase, two limitations exists for the scenarios where high transmit power is required. First, all of the previously cited works are realized with relatively low transmit power (23-24dBm), for instance in [9] and [12], the analog RF cancellation reaches a maximum of 65-70dB. This can be an issue with a high dynamic range system such as a LTE BS transmitting at 46dBm and receiving UE uplink as low as -101.5dBm. A receiver with any transmission over 47.5dBm will be saturated even without having any margin to compensate for PAPR of OFDMA if one assume a 65dB analog cancellation<sup>2</sup>. Moreover, current implementations show

<sup>2</sup>A high quality ADC receiver with 16 bit resolution using 2 bits of margin can only provide a 84dB dynamic range.

that combined analog plus digital cancellation can reach up to 110dB. When using a high transmission power, this leads the received signals to be much higher than the usual sensitivity (around -70/-60dBm for UL) due to the increased noise floor. This will significantly drain the battery of classical UEs and will limit the maximum distance for the backhaul links. This is what can be seen on the estimated crossover points of [6], showing when FD is beneficial over HD depending on the transmitting power. Also [13] shows that the FD approach can greatly increase the performance subject to a smaller coverage.

The second limitation comes from the incompatibility of FD with respect to the legacy UEs as it is not part of the standard and additional procedures are needed on both network and terminal side to support the FD transmission (e.g. assigning different TDD configurations to different UEs). In addition, the problem of joint scheduling inherent to the backhaul network itself with multiple adjacent nodes remains open although FD systems address the joint access and backhaul links sharing.

### C. In-band backhauling

A third option is to re-use the relay channel that allows in-band backhauling between a relay and its DeNB. As the 3GPP relays can connect only to one DeNB, creating a LTE mesh network based directly on them is not possible. However, we advocate that we can share the multiple MBSFN SFs between adjacent BSs and leverage the  $Un$  channel to use these SFs and to interconnect the BSs to create a multi-hop mesh network.

In [2] and [7], we introduced the enhanced evolved Node B (e2NB) as an evolution of the eNB designed to work as a standalone while having meshing capabilities. As a moving standalone cell, an e2NB incorporates part of the core network to be able to handle UEs locally. It also incorporates and manages virtual UEs that share its radio interface, leveraging legacy UE procedures for detection and initial connection to adjacent e2NBs before switching to  $Un$  channels for inter-e2NB communications. This approach only requires new scheduling schemes and some associated procedures. It does not disrupt the service to the legacy UEs and does not require modifications of the physical layer.

1) *Synchronization*: In case of large networks, adjacent e2NBs need to be SF synchronized. Their DL and UL SFs must start and end at the same time, otherwise some links using  $Un$  may not be possible. A simple example with two e2NBs is shown on Fig. 4, where it is not possible to have a  $Un$  channel in both directions with a propagation time in the order of a symbol time (corresponding to around 20km which can be realistic for high powered maritime/PS applications).

2) *Mesh scheduling and interference*: Scheduling in a mesh network based on  $Un$  links sharing MBSFN SFs is more complex than scheduling of relays connected to a single DeNB. It is similar to node scheduling in a TDMA wireless mesh where transmissions between BSs need to be coordinated otherwise leading to blocking issues or interference.

To cope with the scheduling issues, each e2NB includes a Coordination and Orchestration Entity (COE). It is responsible for the scheduling of SFs in the mesh network at two different

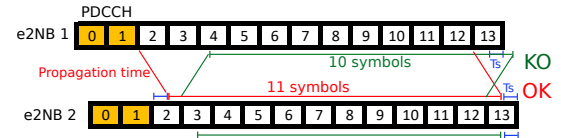


Fig. 4: Transmission problem for non subframe synchronized e2NBs

levels. At a network wide level in a centralized fashion, a COE applies and updates periodically a MBSFN SFs sharing policy to allocate to each e2NB a set of SFs on which said e2NB can transmit. It may rely on a SuperFrame to define sharing of MBSFN SFs for periods longer than a frame. The policy applied depends on the goals of the network: maximize network throughput, respect specific QoS metrics, etc., and needs COEs to cooperate for metric gathering. It can also take into account specific routing policies that can be broadcasted.

Then, at each e2NB and time slot, the COE applies specific rules to the local MAC scheduler that is responsible for the link allocations at each SF thanks to the one-to-multi point transmission capabilities of LTE. These rules can take into account network wide QoS requirements, for instance to prioritize some links or some flows.

### D. Comparison

A comparison of the three above-mentioned LTE meshing solutions is presented in TABLE I. It can be inferred that the in-band  $Un$  approach represents an opportunity to limit the modifications in the PHY/MAC layer and design a joint backhaul and access coordinated scheduling while retaining the flexibility in terms of radio resources sharing between the backhaul and access, the compatibility with the legacy UEs, and the cost of BS.

## IV. EVALUATION OF THE $Un$ CHANNEL

### A. Link-level evaluation

In this section, we compare the performance of the relay physical channels against the legacy LTE physical channels to ensure that the relay interface is efficient on a computing perspective and retains the channel efficiency. OpenAirInterface (OAI), a software-defined LTE platform, is used as an emulated LTE environment for our experimentations.

A subset of R-PDCCH and R-PDSCH functionality is developed in OAI and experimented in DL between a DeNB and a relay node. The subset implements R-PDCCH encoding and decoding of DCI for DL allocation in the first slot and UL allocation in the second slot with resource allocation type 0 mapping over resource elements. It also implements R-PDSCH encoding and decoding with resource allocation type 0. Both support all DL\_StartSymbol and second slot configuration (6 or 7 symbols). An extensive set of experiments has been carried out to analyze the impact of various parameters on link-level performance and computing requirements. To ensure the consistency of the results, all the experiments are single threaded and are performed on the same machine running Ubuntu 14.04.5 with kernel 4.4.0 over an Intel Xeon E5-2640v4 at 2.4GHz running without Hyper-Threading or Turbo.

For each run, a large number of SF transmissions is generated with the same set of parameters over a random AWGN

TABLE I: Comparison of different LTE meshing solutions

BS meshing solution	Out-band $Uu$	Full-Duplex $Uu$	In-band $Uu$
Required frequency bands	Backhaul and access separated	One shared backhaul/access	One shared backhaul/access
Backhaul/access flexibility	Low	Medium	Medium
Scheduling complexity	Medium	Medium to High	Medium to High
Range	+++	+ (limited by RF cancellation)	+++
Hardware Cost	+ to +++ depending on band separation	++	None (TDD) / + (FDD)
Legacy UE support	Yes	No	Yes

channel in a Monte Carlo fashion. The SNR is increased until it satisfies the required 75% successful transmissions.

1) *Computation time*: First, we compare the computation time required to perform R-PDCCH and PDCCH signal generation (TX at DeNB) and decoding (RX at relay) with different aggregation levels. A DCI is 8-57 bits long. To increase its code rate, it is encoded over 72, 144, 288 or 576 bits in aggregation level 0, 1, 2 or 3 respectively. It can be seen from the Fig. 5a that the R-PDCCH encoding and resource element mapping computation time is almost twice as in PDCCH, and that it is independent of the position of DCI in the R-PDCCH VRB set. On the other hand, the PDCCH encoding and mapping computation time increases when the DCI is in the second position as it performs encoding and mapping for two DCIs, which leads to an increase of the number of PDCCH symbols when using the aggregation level 3.

It has to be mentioned that the R-PDCCH generation in this first experiment is always done for a DL DCI format1 in the first slot and a UL DCI format0 in the second slot, while the PDCCH generates only DL DCI(s) format1. Adding a UL DCI for the PDCCH is the same as adding a PDCCH DL DCI, but generating only a DL DCI for R-PDCCH would have cut the R-PDCCH generation time by half. Fig. 5b shows the computation time for the DL PDCCH, and both DL and UL R-PDCCH DCI decoding. It can be observed that the PDCCH decoding computation time is proportional to the number of PDCCH symbols that only increases from one to two in case of the aggregation 3 and DCI position 2. R-PDCCH decoding is faster for small aggregation level but tends to increase with higher aggregation level. We note that the UL R-PDCCH has a smaller decoding time than that of DL when the aggregation level increases. This is because the DL DCI decoding part looks for several DCI formats for each aggregation level while the UL part looks only for DCI format0.

In the next experiment, as we vary the MCS value we compare the total processing time to complete (a) the (D)eNB transmission procedures and OFDM encoding, when using either PDCCH/PDSCH or R-PDCCH/R-PDSCH (no DCI on

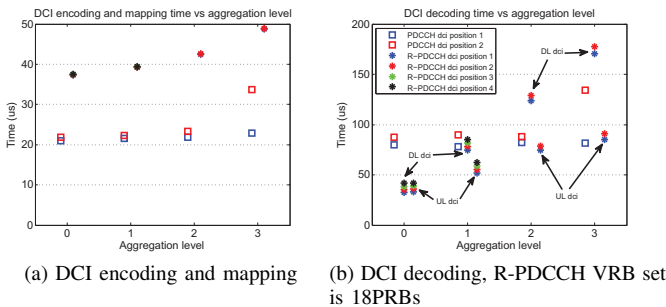


Fig. 5: R-PDCCH and PDCCH computational time for 10MHz channel

PDCCH but other legacy controls channels are included), and (b) relay reception procedures to decode the corresponding control and data channels. A static resource allocation is used, which includes 25 (5MHz channel) and 100 PRBs (20MHz) for the  $Uu$  channel, and 24 PRBs (5MHz channel) and 96 PRBs (20MHz) for the relay channel with a R-PDCCH VRB set containing only one (5MHz) or four (20MHz) PRBs. It can be seen from Fig. 6 that TX procedures take a bit longer at the DeNB for the relay channel. The difference remains almost constant over all MCS values, and it mainly corresponds to the DCI encoding time as presented in Fig. 5. RX procedures at the relay node are slightly faster than the legacy UE, which is due to lower DCI decoding time for R-PDCCH. In addition, the results also reveal that the HARQ deadlines are met for all cases (including 100 PRBs and MCS 28) as the sum of TX and RX processing remains below 3ms [14], which proves the feasibility of a fully software implementation of DeNB and relay node on the commodity hardware.

2) *Link-level performance*: To evaluate the relay DL performance, the signal-noise ratio (SNR) is monitored to obtain 75% of successful transmission for a given transport block size (TBS). Because the resource allocation type 0 has a minimum granularity of 1RBs at 5MHz, 2RBs at 10MHz and 4RBs at 20MHz, and as the allocation on the second slot of the R-PDCCH is not possible (for R-PDSCH) due to our current implementation, the number of available RBs and the resulted TBS is reduced by a minimum of 1/25 of the maximum TBS if we allocate all the available resources to a single user. As the TBS is not linked to the number of available symbols for the PDSCH or R-PDSCH, the actual code rate of a given TBS changes depending on the length of the data channel.

Fig.7 presents the resulted TBS versus the minimum re-

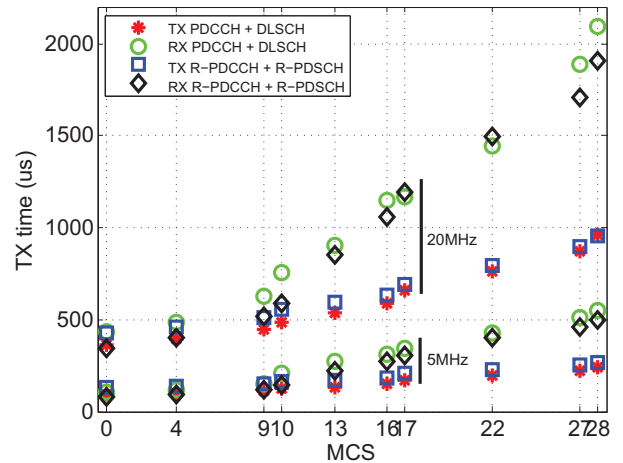


Fig. 6: Total TX and RX processing time for PDCCH/PDSCH and R-PDCCH/R-PDSCH

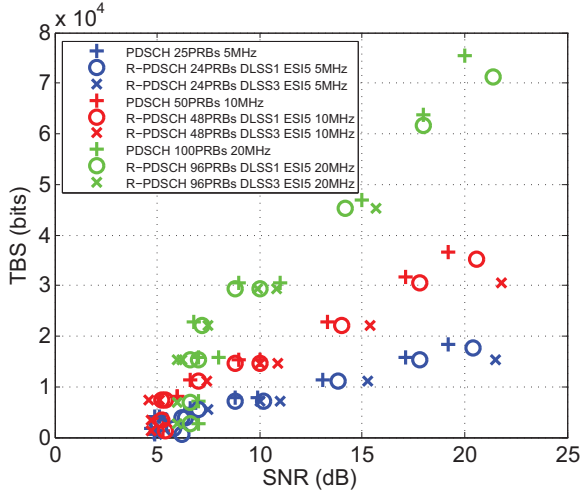


Fig. 7: Minimum SNR to decode 75% of the transmission for different channel bandwidth, DL\_StartSymbol (DLSS) and second slot End Symbol Index (ESI). Maximum PRB allocation for one user. Different TBS values are obtained from different MCS values (0,4,9,10,16,17,22,27,28).

quired SNR as a function of channel bandwidth (25PRB, 50PRBs, and 100PRBs) and modulation and coding schemes (MCS 0,4,9,10,16,17,22,27,28) with (R-)PDCCH aggregation 0. Note that the MCS0 is the bottom-most point and the MCS28 is the topmost point. From the figure, it can be inferred that the efficiency of the R-PDCCH/R-PDSCH is very close to that of PDCCH/PDSCH with slightly lower maximum achievable data rate. In particular when the number of symbols is reduced to 10, the maximum MCS/TBS values cannot be decoded as they lead to a code rate close to or higher than 1.

The achievable performance using different aggregation level is compared in Fig. 8. It can be observed that at low TBS, the required SNR to achieve 75% successful transmissions is similar in both R-PDCCH/R-PDSCH and PDCCH/PDSCH channels, even with a reduction in the available number of RBs (i.e. 2/6/9 less PRBs for R-PDSCH). Starting from 6dB of SNR, the TBS does not increase with the aggregation levels (as aggregation 0 becomes sufficiently robust), and the impact of missing PRBs on the achievable data rate (i.e. reduction

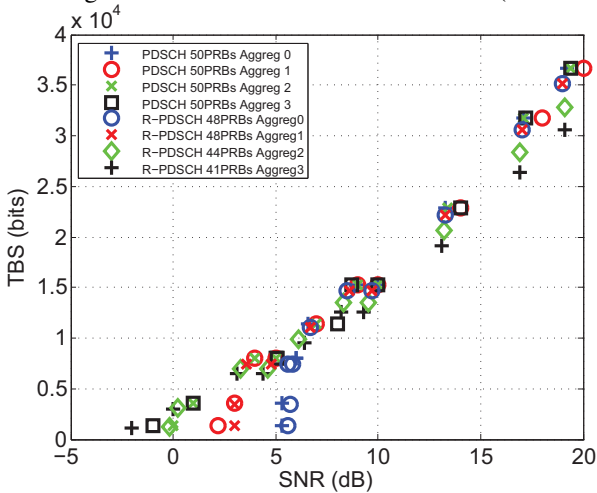


Fig. 8: Minimum SNR to decode 75% of transmissions for different aggregation level. 10MHz channel with maximum PRB allocation for one user. Different TBS values are obtained from different MCS values (0,4,9,10,16,17,22,27,28).

in TBS) becomes significant (the corresponding points in the figure are diverging).

The above results prove that the performance of the relay channel is very close to the legacy  $Uu$  channel, making it a promising candidate for self-backhauling and meshing of LTE BSs as we previously advocated [1], [7].

### B. $Uu$ out-band and $Un$ in-band throughput comparison

In a second experiment, a complete LTE simulator is developed in Matlab allowing to create a 2D-map of an arbitrary network of BSs with their associated UEs and to generate arbitrary flows between every type of nodes. Using that simulator, we compare the achieved throughput of  $Un$  in-band against  $Uu$  out-band when used for self-backhauling.

1) *Topologies and architecture:* A simple topology consisting of three aligned BSs spaced by 3km is simulated. BSs serve UEs in a 1km radius. BSs and UEs are assumed to be fixed over time and equipped with omni directional antennas. As shown on Fig. 9, in the  $Uu$  out-band case, each BS integrates two radios: a) one dedicated to serve their local UEs on Band C, and b) one dedicated for the backhaul on Band B. The backhaul radio acts either has a eNB (BS 2) or as a UE (BS 1 and 3). We assume that each node host a local EPC and some routing service to route the traffic locally or on the backhaul. In the  $Un$  in-band case, each BS is a e2NB as described in [7]. It hosts its own EPC, has a Control and Orchestration Entity (COE) for the backhaul management and uses a unique radio as shown on Fig. 10.

2) *Scheduling algorithm:* In [15], we detailed the role of the COE and proposed a scheduling algorithm to manage the SF allocation for the backhaul/access in the  $Un$  in-band case. We use that algorithm in these simulations. In the  $Uu$  out-band case, there is no need for a specific backhaul scheduler as the backhaul relies on a classical eNB/UEs architecture: the scheduling is ensured by the eNB Band B in BS 2.

3) *Channel models:* Band A ( $Un$  backhaul and  $Uu$  access) is configured to be FDD 10MHz wide while Band B ( $Uu$  backhaul) and C ( $Uu$  access) are configured to be FDD 5MHz wide. This gives the same global bandwidth in both cases. All radios can use up to MCS28 on DL and UL. Band A and B are centered at 2.2GHz while Band C is at 2.3GHz. We assume that there is no interference between band B and band C. Between BSs, a freespace path loss model of coefficient 2.1 is applied with Claussen shadow fading and EPA channel type. Between BSs and UEs (not including UEs that are in BS), a rural (TR 36.942) path loss model is used with Claussen shadow fading and EPA channel type.

4) *Traffic patterns:* First, we consider three separate cases where we generate a unique flow between two specific entities. Then, we generate two flows at the same time to show the dependency between some links. All cases are performed over a 10 seconds (10000 SFs) simulation.

5) *Results:* Fig. 11 presents the data rate of the flow when we generate only one at a time. We can see that for a one hop flow from BS 2 to BS 1,  $Un$  backhaul performs slightly better than the  $Uu$  backhaul. Indeed,  $Un$  can use at maximum

6 SFs per frame for the backhaul (the actual share of SFs and the use of DL or UL SFs is managed by the COE). On a 10MHz bandwidth, it gives roughly 20% more throughput than using 10 UL SFs per frame on a 5MHz bandwidth as the  $Uu$  backhaul does. With a flow transmitted from BS 2 to BS 3 over two backhaul hops, the flow data rate over  $Uu$  backhaul does not change as it is limited by the UL link from BS 2 to BS 1 (PRBs reserved for PUCCH makes it slower than DL).  $Un$  backhaul performs worse because it has to rely on UL SFs for half of its transmissions while it was previously mainly using DL SFs. It also suffers from its slightly lower efficiency compared to  $Uu$  as shown in IV-A2. When transmitting only a flow from UE 1 to BS 1, the  $Un$  backhaul architecture performs much better as almost all the 10MHz bandwidth can be used by the UE for the UL (almost no SFs are reserved for backhaul as there is no traffic) while the  $Uu$  case is limited to 5MHz.

Fig. 12a shows the data rate when we generate two flows: one from UE 1 to BS 1 and one from BS 1 to BS 2. In that case, the COE tends to allocate most of the MBSFN SFs as backhaul DL SFs for BS 1. It allows BS 1 to use almost all its UL SFs to receive either from its UEs or from adjacent e2NBs. As there is no traffic coming from other e2NBs, UE 1 gets the full UL bandwidth, which allows the  $Un$  architecture to perform much better than the  $Uu$  one.

Finally, Fig. 12b shows the data rate when we generate two flows: one from UE 1 to BS 1 and one from BS 2 to BS 1. In such a case, BS 1 is not transmitting but only receiving. While  $Un$  allows more flexibility between the backhaul/access share than  $Uu$ , it still limits the radio to be doing 50% TX and 50% RX in a FDD case. As the COE gives most MBSFN SFs for DL on the backhaul to BS 2, the BS 1 has on average only 4 UL SFs available for its UE. This reduces the UL data rate and puts the global throughput on the network behind the  $Uu$

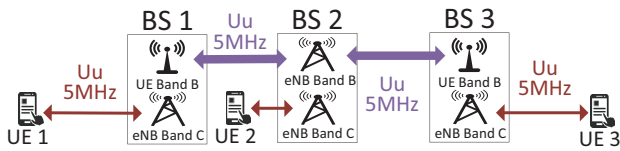


Fig. 9:  $Uu$  out-band self-backhauling topology



Fig. 10:  $Un$  in-band self-backhauling topology

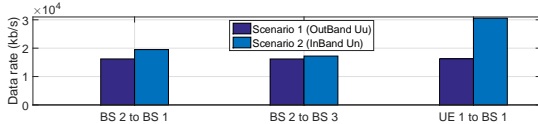
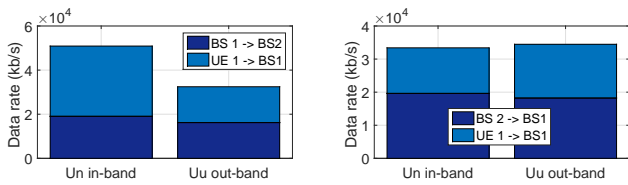


Fig. 11: Data rate of flows in both backhaul architectures



(a) First double flows setup

(b) Second double flows setup

Fig. 12: Stacked data rate of flows in both backhaul architectures

case that has complete backhaul/access separation.

These results show that the  $Un$  interface allows to balance the resources between the access and backhaul links at each node enabling higher throughput for the transmitted flows.

## V. CONCLUSION

In this paper, we present the LTE relay interface ( $Un$ ) and the associated physical channel (R-PDCCH, R-PDSCH). We analyze architecture solutions to realize a LTE mesh network and we compare different approaches including out-band  $Uu$ , full duplex radios, and in-band  $Un$  as LTE backhauling candidates. We then evaluate the performance of the relay physical channels through a link-level emulation. We show that the  $Un$  interface performs close to the legacy  $Uu$  interface regarding computing requirements but that the code rate increase induces a slight data rate drop at equivalent SNR. We finally compare out-band  $Uu$  and in-band  $Un$  self-backhauling approaches over a simple topology and we show that  $Un$  allows for more flexibility on the backhaul and access resource provision enabling higher throughput on most cases.

In future, we plan to finish implementing the  $Un$  interface over OpenAirInterface to realize RF experiments.

## REFERENCES

- [1] R. Favraud *et al.*, "Toward moving public safety networks," *IEEE Communications Magazine*, vol. 54, no. 3, pp. 14–20, March 2016.
- [2] —, "Public safety networks: Enabling mobility for critical communications," in *Wireless Public Safety Networks 2 : A systemic approach*, ser. Wireless Public Safety Networks. ISTE, Jul. 2016, no. 2.
- [3] A. Al-Hourani and S. Kandeepan, "Cognitive relay nodes for airborne lte emergency networks," in *Signal Processing and Communication Systems (ICSPCS), 2013 7th International Conference on*, 2013.
- [4] M. Casoni *et al.*, "Integration of satellite and lte for disaster recovery," *Communications Magazine, IEEE*, vol. 53, no. 3, pp. 47–53, March 2015.
- [5] R. A. Pitaval *et al.*, "Full-duplex self-backhauling for small-cell 5g networks," *IEEE Wireless Communications*, vol. 22, no. 5, pp. 83–89, October 2015.
- [6] J. H. Yun, "Intra and inter-cell resource management in full-duplex heterogeneous cellular networks," *IEEE Transactions on Mobile Computing*, vol. 15, no. 2, pp. 392–405, Feb 2016.
- [7] R. Favraud and N. Nikaiein, "Wireless mesh backhauling for lte/lte-a networks," in *Military Communications Conference, MILCOM 2015 - 2015 IEEE*, Oct 2015, pp. 695–700.
- [8] Y. Yuan, *LTE-Advanced Relay Technology and Standardization*. Springer-Verlag Berlin Heidelberg, 2013.
- [9] D. Bharadia *et al.*, "Full duplex radios," in *Proceedings of the ACM SIGCOMM 2013 conference on SIGCOMM*, 2013.
- [10] S. Goyal *et al.*, "Improving small cell capacity with common-carrier full duplex radios," in *IEEE International Conference on Communications (ICC)*, June 2014.
- [11] —, "Analyzing a full-duplex cellular system," in *Information Sciences and Systems (CISS), 2013 47th Annual Conference on*, March 2013.
- [12] D. Bharadia and S. Katti, "Fastforward: Fast and constructive full duplex relays," in *Proceedings of the 2014 ACM Conference on SIGCOMM*, ser. SIGCOMM '14. New York, NY, USA: ACM, 2014, pp. 199–210.
- [13] A. Sharma *et al.*, "Joint backhaul-access analysis of full duplex self-backhauling heterogeneous networks," *CoRR*, vol. abs/1601.01858, 2016.
- [14] N. Nikaiein, "Processing radio access network functions in the cloud: Critical issues and modeling," in *Proceedings of Mobile Cloud Computing and Services*, ser. MCS '15, 2015.
- [15] R. Favraud *et al.*, "QoS Guarantee in Self-Backhauled LTE Mesh Networks," *Eurecom*, Tech. Rep. RR-17-332, April 2017.